Cytochrome *c* Oxidase: Catalytic Cycle and Mechanisms of Proton Pumping-A Discussion†

Hartmut Michel

Department of Molecular Membrane Biology, Max Planck Institute of Biophysics, Heinrich-Hoffmann-Strasse 7, D-60528 Frankfurt/Main, Germany

Received May 13, 1999; Revised Manuscript Received August 16, 1999

ABSTRACT: Cytochrome *c* oxidase catalyzes the reduction of molecular oxygen to water, a process in which four electrons, four protons, and one molecule of oxygen are consumed. The reaction is coupled to the pumping of four additional protons across the membrane. According to the currently accepted concept, the pumping of all four protons occurs after the binding of oxygen to the reduced enzyme and is exclusively coupled to the last two electron transfer steps. A careful analysis of the existing data shows that there is no experimental evidence for this paradigm. It is more likely that only three protons are pumped during the second half of the catalytic cycle of cytochrome *c* oxidase after the reaction with oxygen. In this article a variant of a recent mechanistic model of proton pumping by electrostatic repulsion is discussed. It is based on the electroneutrality principle in a way that in the catalytic cycle each electron transfer to the membrane-embedded electron acceptors is charge-compensated by uptake of one proton. The mechanism takes into account the findings with mutant cytochrome *c* oxidases and explains the results of many recent experiments, including the effects of hydrogen peroxide.

Cytochrome *c* oxidase (COX)[1] is the terminal enzyme of the respiratory chains of mitochondria and many aerobic bacteria. It couples the oxidation of cytochrome *c*, the reduction of oxygen, proton consumption, and water formation to the electrogenic transfer of up to four additional protons across the mitochondrial or bacterial membrane. It thus pumps protons (*1*) according to

$$4\ \text{cytochrome}\ c^{2+} + 8\ H_i^{+} + O_2 \rightarrow 4\ \text{cytochrome}\ c^{3+} + 4\ H_o^{+} + 2\ H_2O \quad (1)$$

where H_i^+ stands for protons taken up from the inside of mitochondria or bacteria and H_o^+ stands for protons released at the outside. Because cytochrome *c* is located on the outside, a total of eight charges is transported across the membrane. Cytochrome *c* delivers its electron to a binuclear Cu_A center, which is located close to the outer membrane surface. Next the electrons are transferred to a low-spin heme *a* in the membrane, and finally to a heme a_3-Cu_B binuclear center, where oxygen reduction takes place (see refs *2* and *3* for extensive reviews).

It has been of considerable interest to understand the mechanism of this fundamental enzyme. Wikström (*4*) has shown that the electron flow in COX can be partially reversed at high redox potentials. He discovered two intermediates and called them F and P, because he interpreted the F-intermediate[2] with its α-band having an absorbance maximum at 580 nm as being an oxoferryl state of the heme a_3 iron atom and the P-intermediate, absorbing maximally around 607 nm, as a peroxy state with a bound peroxide dianion between the heme a_3 iron and Cu_B. A catalytic cycle was proposed (see, e.g., ref *5*), in which a bound oxygen molecule is reduced to a bound stable peroxide species by electron transfer from the reduced forms of heme a_3 and Cu_B. Then one further electron and two protons are needed to convert the P-state to the F-state, and finally the O-state is reached by consuming a fourth electron and two protons. Such a simple catalytic cycle is shown in Figure 1 (top). In line with this cycle it was postulated that two protons are consumed per P → F and F → O transition (*5*) and that proton pumping is exclusively coupled to the P → F and F → O transitions with two protons pumped per transition (*6*). This widely accepted proposal has been challenged recently, on the basis of the X-ray crystallographic structure analyses of the bacterial (*7*, *8*) and mitochondrial (*9*−*11*) COXs (*12*). First doubts were raised (*13*) upon the finding that only close to one proton per functional COX was taken up when the fully reduced enzyme was oxidized with oxygen [after flashing off bound carbon monoxide (CO)] and not four as would be expected from a catalytic cycle as shown in Figure 1 (top). In addition, the observation was made (*14*) that the reduction of isolated COX is accompanied by the uptake of two protons during the first two electron transfers. The

† Financial support was provided by the Deutsche Forschungsgemeinschaft (SFB 472), the Fonds der Chemischen Industrie, and the Max-Planck-Gesellschaft.

[1] Abbreviations: CO, carbon monoxide; COX, cytochrome *c* oxidase; Δp, electrochemical proton gradient (membrane potential minus 59 mV• ΔpH, with $\Delta pH = pH_{out}$ minus pH_{in}); ENDOR, electron nuclear double resonance; EPR, electron paramagnetic resonance; EXAFS, extended X-ray absorption fine structure; FTIR, Fourier transform infrared; rdl*a*, relative dielectric location of heme *a* in the dielectric barrier of the membrane.

[2] The terms P-state or F-state (-intermediates) will be used in the following just to indicate that the state (intermediate) has (or is expected to have) an absorption maximum at 607 nm (P-states) or 580 nm (F-states) irrespective of its true chemical structure.

10.1021/bi9910934 CCC: $18.00
Published on Web 10/30/1999

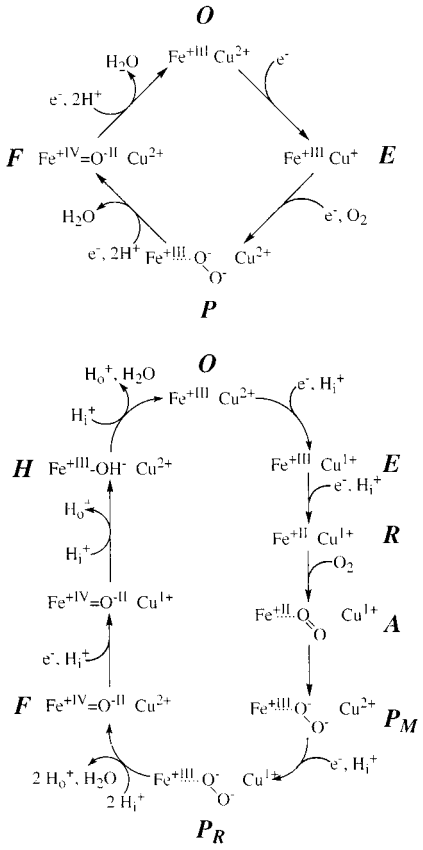

FIGURE 1: Previously proposed catalytic cycles of COX. (Top) Classical model for the catalytic cycle of COX (modified after ref *5*). Only the binuclear site (heme a_3 iron and Cu_B) is shown. The oxidized state O is converted to the one-electron reduced state E. The E-state is reduced by uptake of one further electron and forms the peroxy state P. The P-state takes up the third electron and two protons, the first water molecule is released, and the oxoferryl state F is obtained. The F-state is transformed to the O-state by uptake of the fourth electron and two protons and release of the second water molecule. (Bottom) Revised cycle, modified after ref *16*. The first two electron transfers are accompanied by the uptake of one proton each, and the two-electron reduced R-state is formed. This state binds oxygen and forms compound A and then a first peroxy state P_M. P_M takes up an electron and a (fractional) proton, and another P-state, called P_R, is obtained (*78*). P_R consumes two protons to form the first water molecule and is converted to the F-state. The F-state forms the O-state via the hydroxy intermediate H. Fe stands for the iron atom of heme a_3, Cu for Cu_B, e^- for electron, H_i^+ for protons taken up from the inside of mitochondria or bacteria, and H_o^+ for protons released to the outside.

transition of the two-electron reduced R-state to the P-state is known not to be connected to proton uptake or release (*13*, *14*). If both the interpretations of refs *5* and *6* and the findings of refs *14* and *15* were correct, a net uptake of six (to seven) protons per catalytic cycle would result, as indicated in an accordingly modified, updated version of the catalytic cycle (*16*) of COX (Figure 1, bottom). However, only four protons would be consumed in water formation. The key experiments of refs *13* and *17* as well as those of refs *14* and *15*, in contrast to that of ref *5* and *6*, have found many independent confirmations (see, e.g., refs *18* and *19*). To elucidate the mechanism of proton pumping it is essential to know which electron transfer steps are coupled to proton pumping. A careful analysis of the basis for the view, that only the P → F and F → O transitions are coupled to proton pumping with two protons pumped per transition, is therefore necessary. As will be shown, there is no experimental evidence for this view. On the basis of the available structural data, the results of experiments with site-directed mutants, and careful consideration of the results of electrostatic calculations, a new detailed mechanistic model for the catalytic cycle and the coupling of the individual proton-transfer steps has been presented (*12*). It makes use of the electroneutrality principle of Mitchell and Rich (*15*), which states "that all changes in the binuclear center are made to be electroneutral by protonation changes". This principle has been used to propose a model of proton pumping (*20*) in which each electron transfer is accompanied by uptake of one proton. These protons are trapped in the enzyme and pumped by electrostatic repulsion from the incoming protons consumed during the P → F and F → O transitions. The new model (*12*) suggests that one proton is already pumped during reduction of the binuclear center and will be discussed in greater detail here. It will be shown that many new results are in excellent agreement with this model.

WHICH ELECTRON TRANSFER STEPS ARE COUPLED TO PROTON PUMPING?

Analysis of Thermodynamic Data. In ref *6* the electron flow in COX of isolated rat liver mitochondria was reversed through addition of ATP. ATP is taken up by the mitochondria and hydrolyzed by the ATPase, which establishes (primarily) a membrane potential that reverses the electron flow until equilibrium conditions are reached. A linear dependence of the logarithm of the [P]:[F] (at pH 8.3) and [F]:[O] (at pH 7.2) ratios on the logarithm of the extracellular [ATP]:[ADP]·[P_i] ratio was found with slopes of 0.9−1 and 0.70−0.75, respectively. These results were interpreted to indicate that 3.6−4.0 protons are translocated per P → F and 2.8−3.0 per F → O transition (input parameter 1), because it is likely that 4 protons are translocated per extramitochondrial ATP molecule taken up and hydrolyzed. Further parameters were that two protons are consumed during the P → F transition and one proton during the F → O transition at pH 7.2 (input parameter 2) and that heme a_3 is located in the middle of the membrane dielectric (input parameter 3). Finally, the data were analyzed in terms of a catalytic cycle in which the F → O transition was split into two steps (F → O′ and O′ → O) with proton pumping coupled to the F → O′ transition and a separate uptake of the two substrate protons associated with the O′ → O transition (input parameter 4). The validity of these input parameters is discussed in the following:

Input Parameter 1. In the analysis of ref *6* it is tacitly assumed that the reactions catalyzed by ATPase and COX are in equilibrium. However, within the chemiosmotic hypothesis both reactions are not in direct equilibrium, but the electrochemical proton gradient (Δp) is an obligatory intermediate. For input parameter 1 to be correct, both the ATPase-catalyzed reaction and the COX-catalyzed reaction have to be in equilibrium with Δp. However, there are statements in the literature like "When ATP-hydrolysis is generating Δp a system probably never reaches equilibrium owing to dissipation of Δp..." (*21*). The existence of proton leaks in mitochondria appears to be responsible for this dissipation (see ref *22* and further references therein). Therefore, a certain percentage of the four protons pumped per extramitochondrial ATP molecule hydrolyzed flows back

through the proton leaks and is not available for reversing the COX-catalyzed reactions.

Input Parameter 2. The number of protons consumed per P → F or F → O transition was derived from the linear dependence of log [P]:[F] and of log [F]:[O] on the extramitochondrial pH upon reversal of the electron flow in COX by addition of ATP in the presence of the K^+/H^+-antiporter nigericin. It was thus concluded from the slope of 2 that two protons are consumed during the P → F transition and that two protons are consumed per F → O transition below an extramitochondrial pH of 7.2. Above pH 7.2 the log [F]:[O] dependence on pH was found to be much less pronounced and was interpreted in a way that no protons are consumed above pH 7.2, and that pH 7.2 is the p*K* of two protonatable groups which are accessible from the mitochondrial matrix. Therefore, at pH 7.2 one proton would be consumed per F → O transition. Caused by the presence of nigericin at an extramitochondrial K^+ concentration of 32 mM the *intra*mitochondrial pH was calculated to be 6.8 at an *extra*mitochondrial pH of 7.2 (*5*). This input parameter has the following shortcomings. First, the free energy of ATP hydrolysis is pH-dependent: the apparent free energy is higher at high pH values than at lower ones. With the same leakiness for protons a higher membrane potential would be created at higher pH values, whereas the pH gradient would remain largely unaffected, due to the presence of nigericin. Therefore, the observed pH dependence may be partly caused by changes in membrane potential, and one cannot conclude that two protons are consumed per P → F transition. The true value must be lower. The second problem is the use of an *extra*mitochondrial pH of 7.2 in the experiment of ref *6*, which was performed in the absence of nigericin. It is well-known that under these conditions the *intra*mitochondrial pH is at least 0.5 pH unit more alkaline than the *extra*mitochondrial pH (see ref *22* and references therein). With the arguments of ref *5*, in ref *6*, therefore, a proton consumption of zero and not of one would have to be used at an *extra*mitochondrial pH of 7.2. A consumption of two protons per each P → F and F → O transition also contradicts all measurements using isolated COX, where in each case (e.g., *13*, *18*, *19*) values for proton consumption (just) below one have been reported. The Wikström group also uses a consumption of one proton per transition in a recent report (*23*). They have tried to resolve the discrepancy in an earlier article (*24*) by arguing that two protons are consumed at high Δp but only one in its absence. They even postulated that the P-state contains "two bound 'mobile' protons", the F-state three, and the O-state four of such protons in the absence of Δp, and these would be released to the matrix side upon increasing Δp. This argumentation is unlikely to be correct in the light of the structure of COX (*7*−*11*) and of the strong mutual electrostatic repulsion of protons taken up (or negative charges left behind), as indicated by the results of electrostatic calculations (*25*) and discussed in more detail below. Of course, an effect of Δp on the p*K* of accessible protonatable groups in the membrane should exist. For a very high Δp of 240 mV, the effect on the p*K* of a protonatable group in the middle of the membrane dielectric would be 120 mV, and thus be equivalent to two p*K* units. This effect contributes to the partial reversal of the COX-catalyzed reaction (*4*−*6*) by the increased Δp upon addition of ATP, in the same way as backflow of electrons from the active site to Cu_A and cytochrome *c* is driven by the membrane potential. In the argumentation of ref *24* this effect therefore would be used twice.

Input Parameter 3. As the third input parameter a location of the active site in the middle of the membrane dielectric has been used, based on the classical work of Hinkle and Mitchell (*26*). The results of the structure analyses (*7*−*11*) appeared not to be in a straightforward agreement with this statement (*12*), because heme *a*, heme a_3, and Cu_B are located considerably closer to the outer than to the inner surface (see Figure 2), and the propionate side chains of both heme groups point toward the outer side into a polar region (see ref *8*), whereas below heme *a* the protein interior is very hydrophobic. However, it is not clear how to treat the existence of the water-containing D-pathway for proton transfer (see below) in such a consideration. Experimentally, Hinkle and Mitchell found a dependence of the redox midpoint potential on an applied membrane potential by a factor of 0.43 for valinomycin-induced K^+ diffusion potentials and of 0.50 for uncoupler-induced H^+ diffusion potentials, meaning that an electron would have to cross 43% (or 50% respectively) of the dielectric barrier from the outer side to heme *a*. These values, referred to as relative dielectric location of heme *a* (rdl*a*) in the following, would have to be corrected when the reduction/oxidation of heme *a* would be accompanied by a vectorial uptake/release of protons. The observed small pH dependence of the redox midpoint potential (*26*) of the isolated CO-inhibited beef heart mitochondrial enzyme was quantitated later (*27*) as 9 mV/pH unit, indicating uptake of 0.15 protons upon reduction. The published results concerning the sidedness of proton uptake/release are controversial. Artzatbanov et al. (*28*) interpreted their results with cyanide-treated mitochondria as indicating that heme *a* reduction is accompanied by slow proton uptake from the mitochondrial matrix. Later, the conclusion of additional rapid proton uptake from the opposite side was reached (*29*, *30*). More recently, COX incorporated into liposomes was used, uptake of 0.86 proton from the inside upon reduction of the CO-inhibited enzyme and release of the same number of protons upon heme *a* oxidation to the outside was reported (*31*), thus establishing a simple proton pump without participation of oxygen. However, the high number of protons per electron reported does not agree with the rather small pH dependence of the midpoint redox potential of CO-poisoned COX (*26*, *27*, *30*). A pH-dependent release of 0.2−0.43 proton upon oxidation of CO-poisoned, reduced cytochrome oxidase to the outside in similar experiments was found very recently (*32*). A release of 0.2 protons was attributed to heme *a* oxidation, which is in much better agreement with the pH dependence of heme *a* redox potential. With a fractional proton uptake from the inside of 0.15 H^+/electron upon heme *a* reduction, the rdl*a* value determined to be 0.43 by imposing a K^+ diffusion potential (*26*) would have to be corrected to 0.33, but to 0.5 for proton uptake from the outside. The rdl*a* value of 0.5, as determined from the pH shift-induced H^+ diffusion potential, would have to be corrected to 0.41 if heme *a* reduction were accompanied by proton uptake from the inside but would not have to be corrected for proton uptake from the outside, because the pH-shift effect and the pH dependence of the heme *a* midpoint redox potential would cancel each other. Therefore, after a correction for proton uptake from the outside, the rdl*a* values determined from

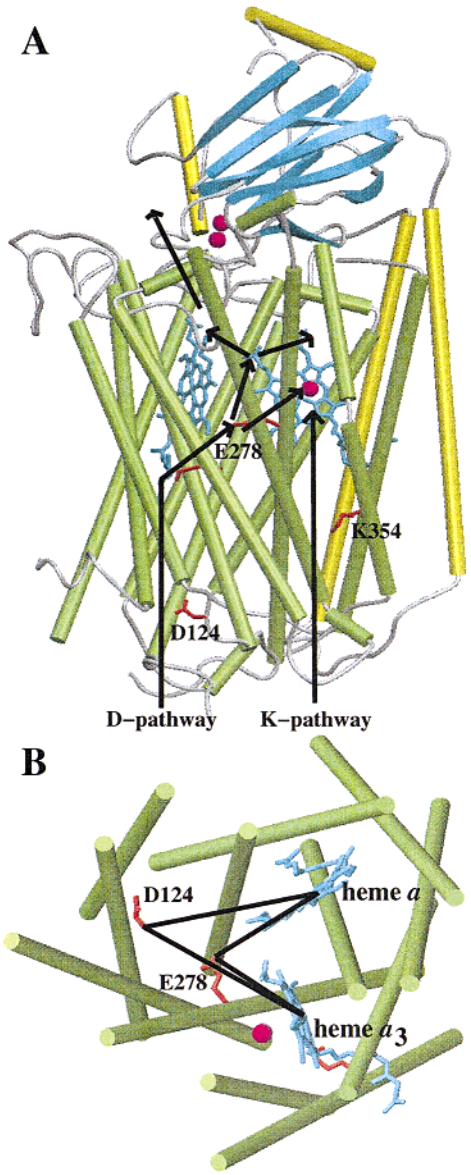

FIGURE 2: Structure of the minimal functional unit of COX. (A) View parallel to the membrane. Helices of subunit I are shown in green, helices of subunit II are shown in olive, and β-strands are shown in blue. The cofactors (Cu_A, two red dots close to the β-strands), heme *a* (blue, left porphyrin), heme a_3 (blue, right porphyrin), and Cu_B (red dot in front of heme a_3) are also shown, as well as the key residues D124, E278, and K354 (shown in red.) The D-pathway of proton transfer leads straight up from D124 and then to E278. Proton transfer continues via the heme D propionate of heme a_3 to the heme *a* propionate area (A in Figure 3) or toward the other heme a_3 propionate and D399 (B in Figure 3). A possible exit pathway is indicated. Proton transfer from E278 to the binuclear site appears to be possible after the formation of P_M in the natural cycle, but after P_R only when P_M has been formed by CO/O_2 treatment (see text). (B) View onto a truncated subunit I from the periplasmic side to show the symmetric location of E278 and D124 with respect to the heme *a* and a_3 iron atoms. Color code is as in panel A.

the K^+ diffusion potential and the H^+ diffusion potential are identical. This finding might either be accidental or indicate that heme *a* is indeed located nearly exactly in the middle of the membrane dielectric, with proton access from the outside. However, for the time being a final answer to this question cannot be given. The rdl*a* value is quite unimportant for the analysis of the thermodynamic data as presented in ref *6* but very important for the interpretation of the results of time-resolved electrometric measurements (see below).

Input Parameter 4. Finally, the data were analyzed in terms of a catalytic cycle (*6*) that uncouples the proton pumping in the F → O transition from the uptake of the two protons needed for the formation of the second water molecule. The existence of an intermediate state O′, suggested to be a dihydroxy state with OH^- groups bound to both the heme a_3 iron and Cu_B, was postulated, with p*K* values of 7.2 for protonation of both groups. Pumping of two protons was assumed to occur between the F- and O′-states and uptake of the two protons for water formation upon transition from the O′-state to the O-state. However, the structural data available now show that the two OH^- groups would come very close together (~2.5 Å distance between both oxygen atoms), resulting in a high electrostatic repulsion. Such a dihydroxy state therefore is unlikely to be a stable, under equilibrium conditions observable, intermediate. Second, protonation of one group would shift the p*K* value of the other by electrostatic repulsion for an incoming proton, making it impossible that both OH^- groups have the same p*K* value (anticooperative effect). The proposed existence of a state O′ was required to explain the dependence of the [F]:[O] ratio on a valinomycin-induced potassium diffusion potential. The dependence of log [F]/[O] was found to be 26.7 mV/decade (*6*), corresponding to transport of 2.2 charges during the F → O transition. It was concluded that this value originates from one electron being transported from cytochrome *c* to heme *a* (0.5 charges) and from pumping of 1.7 protons. A simpler explanation is that 0.5 charges are due to the electron transport, one proton is taken up from the opposite side to maintain electroneutrality around the binuclear site (0.5 charges), and one proton only is pumped, adding up to 2.0 charges, in reasonable agreement with the experimental value of 2.2.

It is important to realize that all proton pump mechanisms in which incoming consumed protons electrostatically repel and thus pump protons during the F → O transition are not compatible with this input parameter 4. These are the published histidine cycle mechanisms (*34*, *35*, *7*), and the electroneutrality-based mechanisms (*20*, *12*).

In summary, it can be stated that the thermodynamic data do not provide any evidence for an exclusive coupling of the P → F and the F → O transitions to proton pumping. In all likelihood three out of the four input parameters are not correct. It may, however, be possible that their shortcomings cancel each other, e.g., if one of the four protons translocated upon hydrolysis per extramitochondrial ATP flows back via the proton leaks, a compensation is possible by the reduction of the number of protons consumed per P → F and F → O transition to one each. But even then the problem with input parameter 4 exists. If input parameter 1 were correct, but only one proton were consumed per P → F and F → O transition (input parameter 2) each, as found with the isolated enzyme, the analysis of ref *6* would result in pumping of three protons per P → F and two or three per F → O transition.

Analysis of Time-Resolved Electrometric Data. Zaslavsky et al. (*35*) were the first to measure the velocity of the generation of an electric field across COX-containing liposomal membranes that were attached to lipid membranes. Using a light-sensitive electron donor, they found a rapid

phase of generation of electric field ($\tau = 45$ μs) and two slower phases ($\tau = 1$ ms and 4 ms) for the F → O transition and interpreted the rapid phase as being caused by electron transfer to heme *a* and the slower phases as being caused by proton uptake and proton pumping. The amplitude of the fast phase was 20% and the sum of the amplitudes of the slow phases was 80% of the overall electrogenic response, resulting in a ratio of 1:4 for the amplitudes of the fast and slow phases. With the parameters of ref *6* a ratio of 1:6 (0.5 for the electron transfer, 2 × 0.5 for consumed protons, plus 2 × 1 for pumped protons) would be expected. Assuming an rdl*a* value of 0.5 and one consumed proton, 1.5 pumped protons were calculated (*35*); with an rdl*a* value of 0.41, this latter value would be reduced to 1.05 pumped protons; and with an rdl*a* value of 0.33, it would be reduced further to 0.66 pumped protons. Therefore, all values are short of the two protons pumped per F → O transition postulated in ref *6*. More recent work with a bacterial COX showed an even higher percentage of the fast phase (*36*), reducing the sum of pumped plus consumed protons further. Jasaitis et al. (*23*) tried to determine the charge translocation stoichiometries using a similar experimental setup, but they started the reaction by flashing off CO from the fully reduced enzyme in the presence of oxygen, thereby creating first a P-state, which is converted to an F-state, and finally to the O-state. They calibrated the relative amplitudes by measuring the electron backflow from heme *a* to Cu_A, which occurs after flashing off CO from a three-electron reduced CO-poisoned COX under anaerobic conditions. With an rdl*a* value of 0.5 the ratio of the amplitudes of the heme *a* → Cu_A electron backflow to the sum of the amplitudes connected to the P → F plus F → O transitions was approximately 1:11, in agreement with one electron transfer to heme *a* plus consumption of one proton plus pumping of two protons per transition. The interpretations have two shortcomings: First, if the rdl*a* value is 0.33, consumption of one proton plus pumping of one proton per transition would fit the experimental data equally well. Second, the calibration procedure was started from a three-electron reduced COX, and the electrogenic phases were ascribed to the electron backflow from heme *a* to Cu_A only. However, the same group has reported very recently (*32*) that oxidation of heme *a* in CO-poisoned COX is coupled to release of 0.2 protons to the outside in approximate agreement with the pH dependence of the heme *a* midpoint redox potential. Therefore, they might have to correct their rdl*a* value of 0.5 to a lower effective value (maximally down to 0.4), to account for the simultaneous release of 0.2 proton to the outside, depending on the location of the proton-releasing site.

Summarizing, one can state that the kinetic data also do not support the claim that the P → F and the F → O transitions are coupled to pumping of two protons each. Then there are two possibilities: either (i) one has to reduce the number of pumped protons per cycle or (ii) one has to attribute some proton pumping to the reductive part of the cycle, because no proton pumping has been observed in the R → P transitions (e.g., *23*). Possibility ii is more likely in the light of the rather strong statement that four protons are pumped per cycle (*37*).

During the revision of this paper, results of electrometric measurements upon addition of a small amount of O_2, starting from a fully reduced enzyme under rereducing conditions, were published (*38*). It was found that ~44% of the transmembrane electric field were generated in the initial oxidative phase and ~56% during rereduction. This result clearly contradicts the general interpretation of the results of ref *6* ("The results show that only two of the electron transfers to the 'peroxy' and 'oxoferryl' intermediates ... are linked to proton translocation ...."), which led to the paradigm that all proton pumping occurs during the oxidative phase. It is now claimed that two protons are pumped during oxidation and two during rereduction but that the proton pumping during the rereduction is linked energetically to the oxidative phase via a high-energy intermediate O~. However, the experiment presented to show that 4 protons are pumped per single turnover of COX indicates pumping of only ~1.2 protons per enzyme upon oxidation without rereduction, whereas upon additional rereduction a total of ~3.8 protons is pumped. Therefore, ~2.6 protons would be pumped during rereduction alone. This result is inconsistent with the claim that two protons are pumped during oxidation and two during rereduction. Actually, there are several indications in the figure presented (figure 2 of ref *38*) that a molar excess of O_2 over correctly oriented COX has been used, leading partially to multiple turnovers (see Supporting Information) and to the much higher apparent proton pumping during rereduction. It must also be noted that the fully reduced state is not part of the natural reaction cycle of COX. It is therefore conceptually incorrect to draw direct conclusions from such an artificial cycle on proton pumping in the natural cycle. The postulate (*6*) that both the P → F and the F → O transitions are coupled to pumping of two protons each is hardly compatible with the new data of ref *38*. In the catalytic cycle O~ follows F and was proposed to decay to the deenergized O, unless it receives an electron within less than 20 s. With the existence of O~ the original postulate of a reversal of O to F and then to P by an imposed membrane potential with equal energy inputs for pumping two protons in the P → F and the F → O transitions each appears to be impossible, because a much higher energy input would be required for the O → F than for the F → P reversal.

STRUCTURE, PROTON TRANSFER PATHWAYS, EFFECT OF KEY MUTATIONS, AND ELECTROSTATIC CONSIDERATIONS

Only subunits I and II are needed for enzymatic activity and proton pumping (*39*). Therefore, further discussions of mechanistic aspects can be restricted to these subunits. Figure 2 shows the structure of subunits I and II of COX from the soil bacterium *Paracoccus denitrificans* (*8*), together with the prosthetic groups, the putative proton-transfer pathways, and three key residues located in these pathways. Cu_A is located in subunit II very close to the periplasmic protein surface, heme *a*, heme a_3 and Cu_B in the upper, periplasmic half of subunit I. The observation that only two potentially proton-accepting amino acid residues are found below heme *a*, heme a_3, and Cu_B is of functional significance. Between the polar protein region at the cytoplasmic surface and the hemes, the only possibly proton-accepting groups are $E278^3$ and K354 (see Figure 2). However, E278 (or the homologous residue) appears to be protonated in the oxidized and reduced states, as deduced from Fourier transform infrared (FTIR) spectroscopy (*40*−*42*), in agreement with the results of the

X-ray crystallographic analyses (*8*, *11*) and electrostatic calculations (*25*). These calculations also indicate that K354 is neutral in the oxidized and reduced states. K354 is a residue within a pathway of proton transfer (*7*, *10*), now called K-pathway (*37*), leading directly to the active site. This pathway also comprises T351, the hydroxy group of the heme a_3 hydroxyethylfarnesyl side chain and Y280. The K-pathway seems to be essential for the reduction of heme a_3 (*37*, *43*), but the reduction of Cu_B upon the first electron transfer is still possible (*44*). K354M mutant enzymes are unable to undergo a complete turnover. They can react with H_2O_2, thereby forming a P-state, and reach the O-state upon further input of electrons (*45*). It was suggested that the K-pathway is not involved in the part of the cycle that leads from the P-state to the O-state (*37*, *43*). This suggestion has been challenged recently, because the turnover with H_2O_2 of K354M mutant enzymes may be slower than that of wild-type enzymes (*46*). However, this issue still has to be settled. The proposal that the K-pathway is used for the first *two* protonations during COX reduction (*43*) appears not to be correct, because there is only one potential proton acceptor, namely, the (putative) OH^- ligand of Cu_B (see below), at the end of the K-pathway. Therefore, only *one* of the first two protons is likely to be taken up via the K-pathway.

The D-pathway starts with D124. It leads straight up to S192 and S193 and then through a presumably water-filled cavity to E278. From E278, proton transfer either to the heme propionate areas (*7*) or to the active site appears possible. D124N and E278C mutant enzymes, as shown for the *Escherichia coli* ubiquinol oxidase (*47*−*49*), possess a similar phenotype: a residual turnover that is uncoupled from proton pumping. E278Q enzymes are completely inactive; the reaction does not proceed beyond the P-state (*48*, *50*, *51*). The location of both D124 and E278 is symmetric with respect to the heme *a* and heme a_3 iron atoms (Figure 2B). Protons therefore would be pulled into the D-pathway electrostatically equally well from an electron at heme *a* and at heme a_3 by electrostatic attraction. It has been suggested that E278 might sense the difference of the net charges between the heme *a* iron atom and the binuclear site (*12*). A COOH group-in contrast to a COO^- group-possesses an electric dipole moment along the line connecting both oxygen atoms. The positive end of the dipole at the OH^- group "likes" to be closer to the more negatively charged metal center. It can do so by a simple rotation around the $C_\gamma-C_\delta$ bond or more pronounced conformational changes. FTIR spectroscopic measurements at 268 K show that the electron backflow from heme a_3 to heme *a* in the two-electron reduced CO-inhibited anaerobic enzyme after flashing off CO causes changes of the vibrational bands of E278 (*52*) in agreement with this proposal. E278 can therefore act as a switch, triggered by electric fields, that possibly connects temporarily established hydrogen-bonded chains leading either to the binuclear site or to the heme propionates. The observation made with the related *E. coli* ubiquinol oxidase, that E286 (homologous to E278) changes its vibrational modes at very low temperature upon flashing off CO under fully reduced, anaerobic conditions (*41*), could not be confirmed with *Paracoccus* COX (*52*). The behavior reported (*41*) for the *E. coli* enzyme was only found with the *Paracoccus* COX, if the enzyme was not fully reduced and allowed to warm. There is therefore no basis for the proposal of a water chain connecting E278 to the binuclear site in the fully reduced COX (*49*). Such water molecules also would have been observed in the refined 2.35 Å resolution structure of the fully reduced bovine COX (*11*) if present. The empty space between E278 and the binuclear site appears to be too narrow to host a chain of water molecules. A structural change would be required first to allow it to build up such a chain of water molecules.

Other proton-transfer pathways have been suggested (*10*). However, the residues of these pathways are not well conserved, and their existence is not supported by any mutagenesis data (*53*, *54*).

The results of electrostatic calculations (*25*) using the coordinates of the *Paracoccus* (*8*) and bovine COX (*10*) have been particularly revealing. They were done in order to identify possibly proton-accepting groups within the protein and to calculate the individual p*K* values of all protonatable residues. Although these calculations reproduce well experimentally determined overall parameters such as the isoelectric point, the uptake of one proton upon single reduction, two protons upon double reduction, and a total of 2.4 protons (*15*) upon further reduction, the assignment of proton uptake to individual amino acid residues is problematic. This is caused by small errors in the coordinates, inhomogeneities of the dielectric coefficient, the strong electrostatic coupling of residues within a cluster above the hemes including the heme propionates, and nonconsideration of possible structural changes during reduction. However, it is clear that protonation of an OH^- group as Cu_B ligand is thermodynamically most favored upon the first reduction. The residual 1.4 protons taken up upon full reduction must be distributed within the cluster of electrostatically coupled residues above the heme groups. The first proton taken up by the cluster electrostatically repels a second proton, explaining why only 2.4 protons are taken up upon full reduction and why the electroneutrality principle is not fully obeyed in the third reduction. The charge-charge interactions between the two heme groups were calculated as ∼2.5 p*K* units (1 p*K* unit equals 60 meV or 1.38 kcal/mol), meaning that reduction of one heme group will change the redox potential of the other by ∼145 mV ("anticooperative effect"). This value is in reasonable agreement with the experimentally determined one of 124 mV (*55*). This result, e.g., also means that addition/release of one proton within the low dielectric environment of COX shifts the p*K* value of another protonatable group at 13 Å distance (the distance between the heme iron atoms) by 2−3 p*K* units. This feature makes it highly unlikely that a high Δp can lead to a release of several (up to four) protons from COX as postulated (*24*). Also intermediates of the catalytic cycles where two negative charges approach each other to less than 5 Å distance without an intervening positive charge are energetically disfavored and should-at least-not be observed as stable intermediates. Such intermediates are dihydroxy states of the binuclear site (like O′ of refs *5* and *6*) or intermediates with an OH^- as Cu_B ligand possessing simultaneously a deprotonated Y280

[3] The sequence numbering of the *Paracoccus* COX is used. D124 corresponds to D135/D132/D91, E278 to E286/E286/E242, Y280 to Y288/Y288/Y244, T351 to T359/T359/T316, and K354 to K362/K362/K319 in the *Escherichia coli* cytochrome *bo* ubiquinol oxidase/*Rhodobacter sphaeroides* COX/bovine heart mitochondrial COX, respectively.

(like P_R in ref *12*, identical to intermediate F_o of refs *19* and *56*). If they exist at all, they must be very short-lived.

MECHANISTIC MODEL OF THE CATALYTIC CYCLE AND ITS COUPLING TO PROTON PUMPING BY ELECTROSTATIC REPULSION

O-State. Special care has to be taken to start with the correct structural model for the oxidized state. This is not straightforward, because the X-ray structures of the O-state only show continuous electron density between the heme a_3 iron and Cu_B (*8*, *11*). This density has been modeled as a peroxide in bovine COX (*11*), which appears to be unlikely in the light of the available spectroscopic information, and as a Cu_B-bound OH^- and a water as a sixth heme a_3 iron ligand in the *Paracoccus* COX (*8*). Evidence for a water or an OH^- group as a Cu_B ligand has been provided by a combination of EXAFS and ENDOR spectroscopy (*57*). A negatively charged ligand must be present, because otherwise an enormous electrostatic repulsion would exist between both metals and destabilize the entire COX. Also, a negatively charged ligand is needed to account for the strong antiferromagnetic coupling between both metals observed by EPR spectroscopy. Even with the OH^- one has to wonder how the existing charge at the heme a_3 iron (formal charge +III, real charge +1) and the remaining charge at Cu_B of +1 can be neutralized. Charge stabilization by protein dipoles has not been observed (*25*). However, the charge at the iron is likely to be compensated by distribution of a partial charge over its histidine ligand, and the residual partial charge can be stabilized by interaction with the heme a_3 propionates, as indicated by the strong electrostatic coupling (*25*). Similarly, the positive charge at Cu_B can be compensated by distributing partial charges over the three histidine ligands and by electrostatic coupling with the heme a_3 propionates and D399. The electrostatic calculations provided no hint that one of the histidine ligands is present in its imidazolate form (*25*). Evidence for a water as the sixth ligand of the high-spin heme has been provided by Cheesman et al. (*58*) for the *E. coli* enzyme. Therefore, the scheme in Figure 3 starts with an O-state consisting of the heme a_3 iron, a water ligand, an OH^- bound to Cu_B, and Y280. The latter appears to be covalently cross-linked to the Cu_B ligand H276 (*11*, *8*). In each state, the heme *a* iron appears on the left. A^- and B^- stand for two clusters of residues (which are subclusters of the cluster identified in ref *25*) that could become protonated upon reduction of heme *a* (A^-) or the binuclear site (B^-). A and B are not individual residues; A should comprise at least the heme *a* propionates, B the heme a_3 propionates and D399. Direct proton transfer from BH to the binuclear site has to be excluded. One now can simply ask what would happen upon sequential addition of electrons to the system under strict consideration of the electroneutrality principle and taking into account the reported properties of the enzyme.

Reduction Phase. The electrostatic calculations (*25*) show clearly that the OH^- ligand at the end of the K-pathway is the thermodynamically most favored acceptor for the uptake of the proton that accompanies the first electron input into the enzyme. However, published statements that the entrance of the D-pathway-in contrast to that of the K-pathway-is surrounded by proton-collecting antennae (*43*) and that the D-pathway site is rapidly protonated whereas protonation of the K-pathway is a long continuous process (*59*), have led to the proposal that the first proton uptake is kinetically driven and occurs via the D-pathway towards the A and B clusters (Figure 2), and a subsequent slower proton uptake via the K-pathway (thermodynamically driven) would later electrostatically repel and thus pump the proton taken up first (*12*). Yet, our recent results (M. Ruitenberg, A. Kannt, K. Fendler, E. Bamberg, B. Ludwig, and H. Michel, unpublished results), using electrometric techniques and pathway mutants, indicate that the first proton uptake occurs via the K-pathway and the second one most likely via the D-pathway. The results do not exclude the possibility of proton pumping after the second electron transfer. The result of the first electron transfer, as indicated in Figure 3, is thus an E-state with Cu_B reduced and its OH^- ligand converted to a water molecule. After the second electron transfer and net uptake of one proton, the R-state of Figure 3 with a proton in the B-site will be reached. A reduction of heme a_3 by the second electron transfer would be impossible, due to the electrostatic repulsion from the already reduced Cu_B, unless this repulsion would be canceled by protonation of the OH^- ligand of Cu_B. This is the reason that, in K-pathway mutants, reduction of heme a_3 is inhibited (*44*, *43*). Next, molecular oxygen will bind to the reduced binuclear site and compound A is formed (*60*).

P_M-State. Compound A spontaneously rearranges without net uptake or release of protons to the P_M-state. On the basis of an analysis of optical spectra, Weng and Baker (*61*) were the first to suggest that the P-state is not a peroxy state but an oxoferryl state with an OH^- bound to Cu_B. They suggested that a tryptophan residue is the source of the missing electron in analogy to cytochrome *c* peroxidase. Later Kitagawa and co-workers (*62*, *63*) provided evidence by Raman spectroscopy that the P-state is a hydrogen-bonded oxoferryl state. Following the original proposal that the covalent cross-link of Y280 and H276 might be the source of the missing electron (*8*), the structure of P_M shown in Figure 3 has been proposed several times (e.g., refs *54*, *64*, *12*, and *56*). P_M will spontaneously form the state F′ shown in Figure 3 by uptake of a proton via the D-pathway, provided the connection from E278 to the binuclear site is established. Protonation via the K-pathway seems not to be possible, because the presence of the neutral tyrosine radical may interrupt the K-pathway (*54*). The uptake of the proton will lead to electrostatic repulsion of the proton in the B-site, and thus pumping of one proton. F′ is thermodynamically much more stable than P_M, because the charge-compensating proton is much closer to the introduced negative charge in F′ than in P_M. The state F′ of Figure 3 has been called F′ [4] according to ref *66*, as it can also be formed directly by reaction of stoichiometric amounts of H_2O_2 with the O-state at low pH (see below). This F′-state has also been termed CcO580 (*67*).

Evidence for a Tyrosine Radical. The existence of the covalent tyrosine-histidine cross-link should be taken as evidence that a tyrosine radical is formed during the catalytic cycle of COX, because cross-linking of tyrosines is typical of a radical reaction catalyzed by peroxidases (see e.g., ref *68*). The tyrosine radical in the P_M-state might not be detectable by EPR spectroscopy, due to antiferromagnetic

[4] Unfortunately, the term F′ has now also been used for an oxoferryl state where Cu_B has a charge of +1 and Y280 is not a radical (*65*).

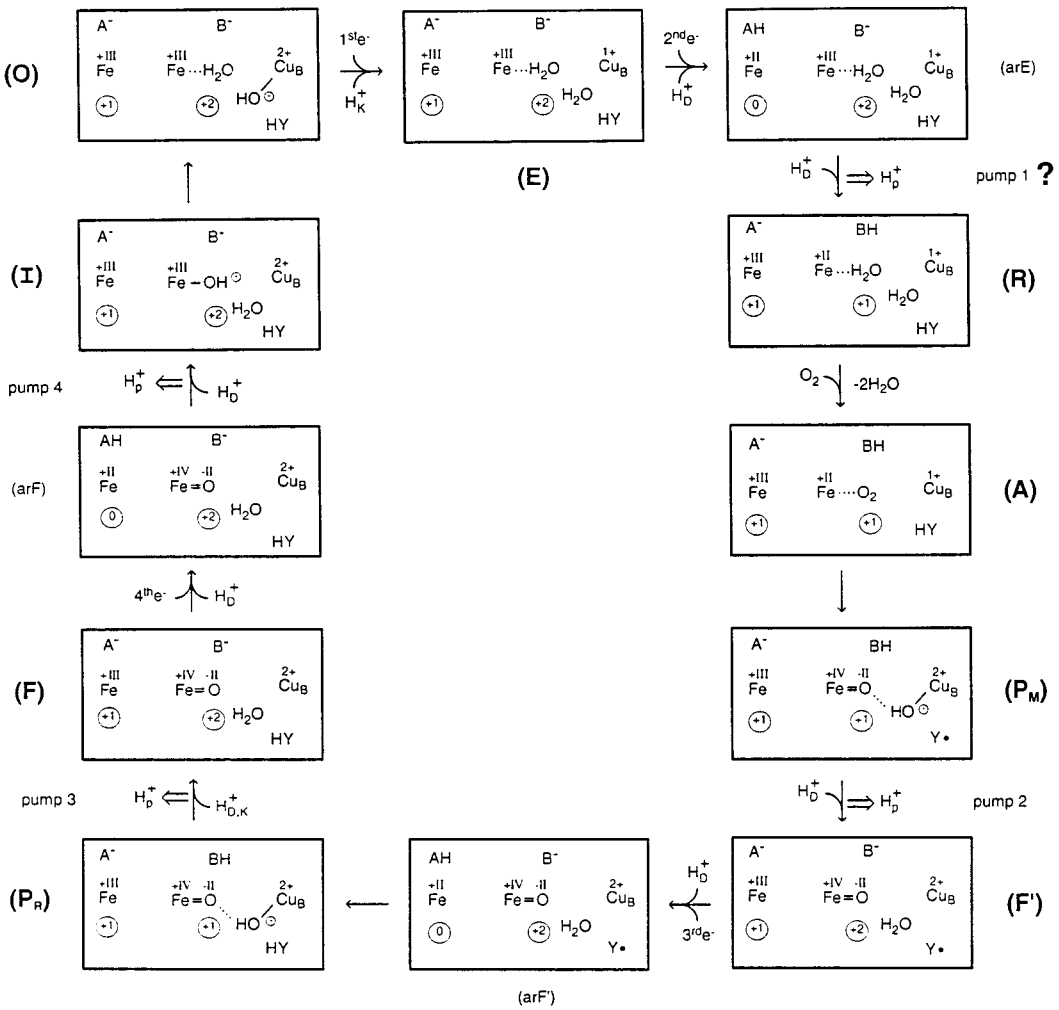

FIGURE 3: Mechanistic model for the catalytic cycle of COX and its coupling to proton pumping by electrostatic repulsion. The left heme Fe symbol in each state stands for the heme *a* Fe atom with +III or +II as its formal oxidation number. A^- stands for a proton-accepting site at the heme *a* propionates. The Fe symbol more to the right stands for the heme a_3 iron. A water molecule (H_2O) is bound to it in the O-state. An OH^- bound to Cu_B is shown. B^- stands for a common protonation site near the heme a_3−Cu_B binuclear site. For each state the overall net charge at the heme *a* Fe site (without A) is indicated within the left-hand circle, and the net charge in the immediate vicinity of the binuclear site (including HY, without B) is shown within the right-hand circle. All changes in the boxes are electroneutral. The reductions of heme *a* during the E → R, F′ → P_R, and F → O transitions are charge-compensated by proton uptake via the D pathway; these protons are stored in the proton-accepting site A. The resulting states are called *a*rE, *a*rF′, and *a*rF, respectively, where *a*r stands for heme *a* reduced. The proposal of a pumping step between *a*rE and R is highly speculative; it might be achieved by electrostatic repulsion of the proton in the A-site by a proton entering the B-site via the D-pathway, if proton transfer from the A-site to the B-site is interrupted. e^- stands for electrons transferred from Cu_A to heme *a*. Protons taken up via the K-pathway are shown as H_K^+, those taken up via the D-pathway as H_D^+, and those taken up via the D- or the K-pathway as $H_{D,K}^+$. Proton pumping is indicated by a double arrow. Y• stands for the neutral radical of the H276−H280 cross-link, and $Y^\ominus$ for the tyrosinate. For more details see text.

coupling by the OH^- ligand of Cu_B (*61*). However, this antiferromagnetic coupling might no longer exist in the F′-state, and the tyrosine radical would become EPR-visible. We could recently show that formation of F′ by treatment with stoichiometric amounts of H_2O_2 at low pH (see below) leads to the appearance of an EPR signal caused by a protein radical and demonstrate that the signal is derived from a tyrosine radical after incorporation of isotopically labeled tyrosine into COX (*69*). Whether Y280 is the responsible tyrosine still has to be finally demonstrated. The EPR invisibility of the (putative) tyrosine radical Y280• in the P_M-state has recently been attributed to spin coupling via the covalently linked Cu_B ligand H276 (*64*). However, Y280 and H276 maintain separate π-electron systems that are not coplanar. This geometry is not optimal for exchange interactions and spin coupling. One also has to keep in mind that three paramagnets (heme a_3 iron, Cu_B, and Y280•) are close together so that predictions are difficult to make. Nevertheless, uptake of a proton that neutralizes an OH^- group into the center of all three paramagnets may alter their coupling to such an extent that the tyrosine radical becomes EPR-visible. It should be remembered that an unassigned protein radical has been observed in COX from bovine heart under turnover conditions in up to 10% of all COX complexes (*70*). If this protein radical can be shown to be a tyrosine radical, strong evidence for this part of the catalytic cycle of Figure 3 would be provided.

Why then can a stable P-state be observed after treatment of a mixed-valence CO-inhibited COX with O_2? One should keep in mind that in this case the two reducing equivalents and two protons are generated inside the enzyme by a chemical reaction ($CO + H_2O \rightarrow CO_2 + 2H^+ + 2e^-$), most likely at the binuclear site. Whereas the electrons will reduce heme a_3 and Cu_B, only one proton binding site is available

at the binuclear site, namely, the OH^- ligand of Cu_B. The other proton has to leave the "reaction chamber". This proton may end up in the wrong position and disturb the hydrogen-bond patterns in the proton-transfer pathways. It is suggested here that the connection between E278 and the binuclear site may not be open when the P-state is generated by CO/O_2 and may be sluggishly open when it is generated by addition of stoichiometric amounts of H_2O_2 (see below).

P_R - and F-State. Next, the third electron transfer to heme *a* would pull in a proton (via the D-pathway) for charge compensation. The proton would probably be stored around the heme propionates. Transfer of the electron to the Y280 radical would convert the latter to a tyrosinate. It is likely that Y280 has a higher p*K* than the Cu_B-bound H_2O/OH^-. Therefore, immediate transfer of a proton from the water to the tyrosinate would occur, and a P-state, called P_R,[5] is formed. A negative charge will be stabilized much more by $Cu^{2+}{}_B$ at the Cu_B ligand than at the tyrosine! The Cu_B-bound OH^- in P_R would receive a proton via the D-pathway (or the K-pathway considering ref *46*). This proton would electrostatically repel and thus pump the proton from BH. As for the $P_M \rightarrow F'$ transition, the driving force is the difference of the p*K* values of the Cu_B-bound H_2O/OH^- and the proton-accepting residue in the B-cluster BH. Thus the F-state is formed, the structure of which seems to be generally accepted.

From F- to O-State. The transition starts again with the transfer of an electron to heme *a*, a charge-compensating proton uptake via the D-pathway, and storage of this proton around the heme propionates. This proton will be pumped later. Upon transfer of the electron to heme a_3 another proton will be pulled in via the D- or K-pathway simultaneously and convert the oxoferryl group to a ferric hydroxy group. The incoming proton again would electrostatically repel (and thus pump) the proton around the heme propionates. The observable intermediate should possess an OH^- group at the heme a_3 iron (*71*) and water at Cu_B (called I, for inverted hydroxy, in Figure 3), which then forms the O-state again by proton transfer from the water to the OH^-. The existence of an observable dihydroxy intermediate is less likely, because the two negatively charged groups would come too close together. The two negative charges would be further apart in a ferric hydroxy/tyrosinate intermediate, making such a structure energetically more favorable than a dihydroxy structure, but such a structure is still not very likely. The existence of the I-intermediate would not exclude the existence of a dihydroxy or a ferric hydroxy/tyrosinate intermediate, if transiently formed, because proton pumping would occur *after* formation of a dihydroxy or a ferric hydroxy/tyrosinate intermediate but *before* the formation of the I-intermediate.

The cycle in Figure 3A of ref *12* cannot be considered to be a viable alternative to that of Figure 3B of ref *12*, as presented here in Figure 3, because the P_R-state[5] there contains the OH^- and tyrosinate close together. In addition, both the A^- and B^- positions cannot be loaded with one full proton each at the same time, due to electrostatic repulsion. If that cycle were used, the total yield of proton pumping from P_M to O could only be 2.4−2.5.

[5] Note that the state called P_R here was termed P'_R in ref *12*.

The cycle of Figure 3 extends the electroneutrality principle to heme *a* reduction. The pumping steps in the $P_M \rightarrow F'$ and $P_R \rightarrow F$ transitions are nearly identical. The cycle explains why P_M and P_R as well as F′ and F have identical optical absorption spectra. The only difference between the two F-states, and between the two P-states, is the presence or absence of a neutral tyrosine radical versus absence or presence of a neutral tyrosine. This difference is unlikely to significantly influence the optical absorption properties of the heme a_3 macrocycle. In this catalytic cycle the last two electron-transfer steps are each coupled to pumping of one proton only!

Effects of H_2O_2. Treatment of oxidized COX with stoichiometric amounts of H_2O_2 leads predominantly to a P-state at high pH but to the F′-state at low pH (*67*). This observation can be rationalized by assuming that at high pH one of the two protons carried into the binuclear site with H_2O_2 is removed from the binuclear site and that the other will be released as water. This P-state is identical to the P_M-state. Without removal of one proton from the reaction chamber, F′ of Figure 3 would be generated directly via a short-lived true peroxy intermediate. The P-state obtained upon addition of stoichiometric amounts of H_2O_2 in *Paracoccus* COX at high pH decays within minutes to F′. This decay is substantially accelerated upon lowering the pH (A. Kannt, and H. Michel, unpublished results). This property was actually used when the presence of a tyrosine radical in F′ was demonstrated (see above). The transition cannot be reversed by increasing the pH again. This observation is in full agreement with the cycle of Figure 3 and a sluggish connection between E278 and the binuclear site, when the P_M-state is generated by H_2O_2. When an excess of H_2O_2 is used, the tyrosine radical in the F′-state might directly react with a second H_2O_2 molecule resulting in the formation of a true F-state and a superoxide radical; the tyrosine radical in the P_M-state might also react with a second H_2O_2 molecule to form the P_R-state and a superoxide radical. The P_R-state would then be converted to the F-state as shown in Figure 3. The proposed relations between the H_2O_2-generated states are visualized in Figure 4 for clarity.

AGREEMENT WITH RECENT EXPERIMENTS

Mutant Data. The results with site-directed mutants are in perfect agreement with the cycle presented in Figure 3. As outlined and explained above, in K354M enzymes heme a_3 reduction is inhibited, due to electrostatic repulsion of the incoming electron by the reduced Cu_B. This repulsion is relieved in wild-type COX through uptake of a proton via the K-pathway, which is not possible in these mutant enzymes. The catalytic cycle in E278Q enzymes does not proceed beyond the P-state (*48*, *50*, *51*), because the proton transfer from E278 to the active site is impaired during the $P \rightarrow F$ transitions. However, a recent further characterization of the E278Q mutant enzyme (*72*) shows that the O-state of this enzyme is unable to react with CO, so the combined treatment with CO/O_2 does not lead to a P-state. As outlined above, one of the two protons produced in the reaction of CO with the enzyme has to be removed from the reaction chamber. These recent results indicate that E278 is involved in the removal of this proton, which is impossible in the E278Q mutant enzyme. The analogous result (*72*) that H_2O_2 treatment of this mutant enzyme does not lead to the

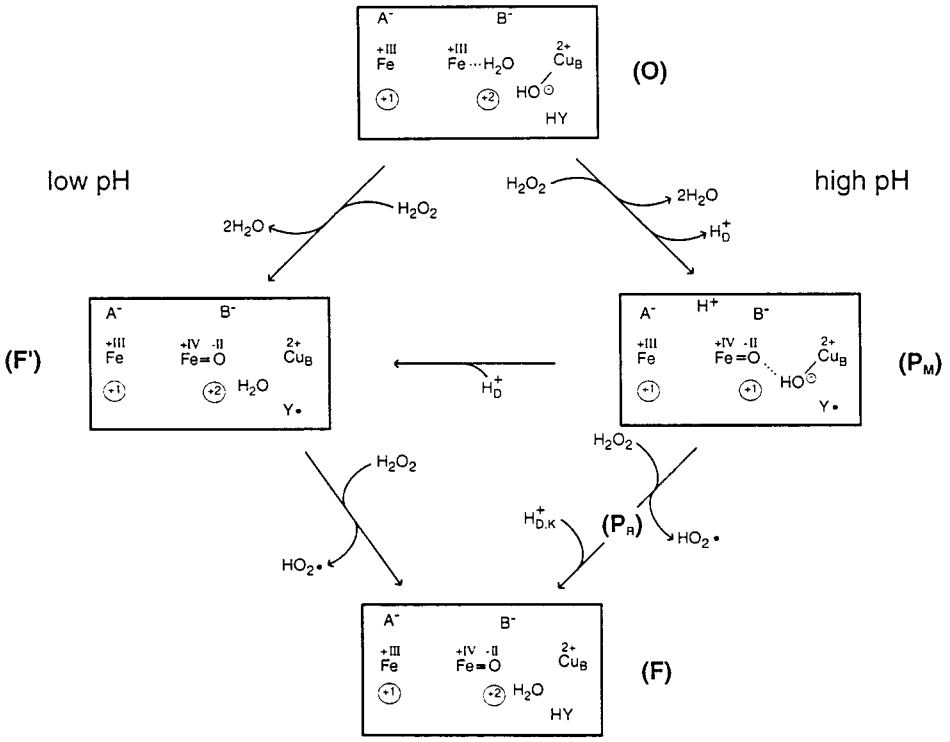

FIGURE 4: Proposed relations between the O-state and the H_2O_2-generated states of COX. Symbols are as in Figure 3. For details see text.

formation of a P_M-state finds the same explanation. The observation that E278Q enzymes accumulate a P-state when the fully reduced enzyme reacts with O_2 but not when the oxidized enzyme reacts with CO/O_2 or H_2O_2 are fully compatible. Within the mechanistic model presented, E278 is needed to allow a proton to access the reaction chamber during the P → F transitions when the reaction has been started by O_2 from the fully reduced state (full reduction has been achieved by artificial electron donors), whereas it is needed to allow a proton to escape from the reaction chamber in the reaction of CO or H_2O_2 with the oxidized enzyme.

D124N mutants are unable to pump protons but show considerable residual activity. This residual activity can be explained by proton backflow from the exit pathway to E278 and then to the binuclear center. This proton backflow and the residual activity will be stimulated by a Δp as observed (*46*).

There are some exotic cytochrome *c* oxidases such as the *ba*$_3$-type COX from *Thermus thermophilus*, where the D-pathway residues D124 and E278 are replaced by aliphatic residues whereas K354 is replaced by a threonine. The K-pathway may still operate, whereas a functional replacement for the D-pathway would be required. The observation that the *ba*$_3$-type COX from *T. thermophilus* pumps protons, but with a stoichiometry of only ~0.5 protons/electron (*73*), might indicate that proton uptake toward the heme propionate areas from the cytoplasmic side via alternate pathways may be rather inefficient.

Spectroscopic Experiments. The demonstration of a tyrosine radical in F′ is in full agreement with the cycle of Figure 3 (see above). In addition, redox FTIR difference spectroscopy with COX preparations specifically ^{13}C-labeled at the heme propionates indicates the existence of structural or protonation changes at the heme propionates (*74*) upon reduction, as required for the cycle of Figure 3.

Results using the flow-flash technique, when the COX reaction is started by flashing off CO from the fully reduced CO-inhibited enzyme in the presence of oxygen, have been interpreted to indicate that proton uptake controls electron transfer in COX (*51*, *75*). This interpretation appears to contradict the cycle in Figure 3 where each electron transfer drives the uptake of one proton and not *vice versa*. However, it is evident from the small pH dependence of the heme *a* redox potential that the fully reduced CO-inhibited enzyme is out of electrostatic balance, because three electrons are in the transmembrane part of the protein, which are charge-balanced by 2.15 protons only, which means that 85% of the reduced enzyme contains 2 protons and 15% contains 3 protons. After the reaction is started, the third electron from heme *a* has to be transferred to the binuclear site and in 85% of the enzyme the third proton has to be taken up before the fourth electron can be transferred to heme *a*, otherwise the electron would be electrostatically repelled. It is therefore the third proton uptake that has to precede the fourth electron transfer. This result is fully in line with the cycle of Figure 3 and the electroneutrality principle.

Electrometric Measurements. The electrostatic imbalance of the CO-inhibited fully reduced enzyme also has consequences when electrometric measurements are performed, starting the reaction by flashing off CO in order to allow oxygen to react with the enzyme. As outlined above, 85% of the COX molecules will be loaded with two protons only. After the flash and generation of a P_M-state, the electron from heme *a* will be transferred to the binuclear site as found (*75*). This electron transfer will open the connection between E278 and the binuclear site, and a proton will be pulled in via the D-pathway into the binuclear site. The electron and the proton will directly convert P_M of Figure 3 into P_R without pumping of a proton. A proton will then be pumped during the P_R → F transition. Therefore, only one proton is pumped during the entire P_M → F transition when starting from the

fully reduced CO-inhibited state, and the other proton is pumped during the F → O transition, resulting in approximately equal amplitudes of the electrometric signals during the P_M → F and F → O transitions, as observed (*23*), and pumping of only two protons during the entire oxidative phase. The very recent observation (*38*) that only ~44% of the electric field is generated during the oxidative phase when starting from the fully reduced state is consistent with the mechanistic model proposed here. Upon full reduction, three electrons are transferred to heme *a*, heme a_3, and Cu_B, leading to transport of 1.5 charge equivalents with an rdl*a* value of 0.5. The reduction would be accompanied by uptake of one proton in order to neutralize the OH^- at Cu_B (0.5 charge equivalent), a second proton would be taken up and transported toward the heme propionate areas, thereby crossing a larger part of the membrane dielectric (~0.75 charge equivalents), and one proton would be pumped. Together ~3.75 charge equivalents would be transported across the membrane during full reduction, leaving only ~3.25 (~46%) charge equivalents for transport in the oxidative phase. This value is within the error margin of the experiment of ref *38*.

Loss of one proton pumping step will also occur when one starts with a P_M-state generated by treatment of a mixed-valence CO-inhibited enzyme with O_2 (*76*). As argued above, the proton-transfer pathway between E278 and the binuclear site might not have been established in this case. Transfer of the third electron to heme *a* will pull in only a small number of protons (0.15/e), due to the electrostatic repulsion from the proton already taken up. The majority of the enzyme will then be in the same state (with respect to heme *a* and the binuclear site, not with respect to Cu_A) as if starting from the fully reduced CO-inhibited form (see above), resulting in pumping of one proton each during the P_M → F and F → O transitions. Therefore, all recent experiments can easily be explained within the cycle of Figure 3, strictly adhering to the electroneutrality principle.

ALTERNATIVE MECHANISMS

Most mechanisms have been based on the assumption that two protons are pumped during the P → F and F → O transitions, and the likely existence of an OH^- group at Cu_B was neglected. Histidine cycles were proposed in order to account for the assumed pumping of two protons in each of these steps (*34*, *35*, *7*). Rich's first mechanism (*20*), based on his electroneutrality principle, also assumed pumping of two protons per transition. His recent variant (*77*), much less detailed than the mechanism presented here, involves accumulation of three protons above the hemes, which is highly unlikely in light of the structures and the results of the electrostatic calculations. It also suggests that E278 acts as a trap. A physical trap appears to be unnecessary, because electric fields, e.g., electrostatic attraction by the reduced metals, and electrostatic repulsion from incoming protons trap the protons taken up first. If E278 were a trap one hardly could explain the observation that imposing a Δp activates D124N enzymes (*46*).

Recently, structural differences between the oxidized and reduced forms of bovine COX around D51 in the loop connecting transmembrane helices I and II, with an orientation of D51 toward the outside in the reduced form, have been observed (*11*). This observation led to the proposal of a mechanism that includes proton release to the outside upon reduction and reprotonation of D51 involving the (unlikely) tautomerization of a peptide bond. Since D51 is only found in COX of animals, the mechanism would not be general. The observation of different positions of D51 in the reduced and oxidized bovine enzyme may find the following explanation: In the orientation toward the protein interior in the oxidized enzyme D51 might carry a negative charge stabilized by accepting three hydrogen bonds as published (*11*). When the enzyme is fully reduced, the electron uptake by Cu_A (distance only 6.7 Å!) will electrostatically repel D51 from its inside position. If this explanation is correct, the structural change will not be present in the two- and three-electron reduced enzymes.

Finally, no plausible mechanism has been suggested how uptake of one proton can drive the pumping of two protons. There is no driving force for preloading two protons, which, in addition, would electrostatically repel each other.

ACKNOWLEDGMENT

I thank J. Behr, A. Harrenga, A. Kannt, and C. R. D. Lancaster for discussion; D. Vinzenz, A. Harrenga, and A. Kannt for preparing the figures; and A. A. Konstantinov, M. Saraste, and P. R. Rich for valuable hints.

SUPPORTING INFORMATION AVAILABLE

A detailed analysis of Figure 2 from ref *38*. This material is available free of charge via the Internet at http//pubs.acs.org.

REFERENCES

1. Wikström, M. (1977) *Nature (London) 266*, 271−273.
2. Ferguson-Miller, S., and Babcock, G. T. (1996) *Chem. Rev. 7*, 2889−2907.
3. Michel, H., Behr, J., Harrenga, A., and Kannt, A. (1998) *Annu. Rev. Biophys. Biomol. Struct. 27*, 329−356.
4. Wikström, M. (1981) *Proc. Natl. Acad. Sci. U.S.A. 78*, 4051−4054.
5. Wikström, M. (1988) *Chem. Scr. 28A*, 71−74.
6. Wikström, M. (1989) *Nature (London) 338*, 776−778.
7. Iwata, S., Ostermeier, C., Ludwig, B., and Michel, H. (1995) *Nature (London) 376*, 660−669.
8. Ostermeier, C., Harrenga, A., Ermler, U., and Michel, H. (1997) *Proc. Natl. Acad. Sci. U.S.A. 94*, 10547−10553.
9. Tsukihara, T., Aoyama, H., Yamashita, E., Tomizaki, T., Yamaguchi, H., Shinzawa-Itoh, K., Nakashima, R., Yaono, R., and Yoshikawa, S. (1995) *Science 269*, 1069−1074.
10. Tsukihara, T., Aoyama, H., Yamashita, E., Tomizaki, T., Yamaguchi, H., Shinzawa-Itoh, K., Nakashima, R., Yaono, R., and Yoshikawa, S. (1996) *Science 272*, 1136−1144.
11. Yoshikawa, S., Shinzawa-Itoh, K., Nakashima, R., Yaono, R., Yamashita, E., Inoue, N., Yao, M., Fei, M. J., Libei, C. P., Mizushima, T., Yamaguchi, H., Tomizaki, T., and Tsukihara, T. (1998) *Science 280*, 1723−1729.
12. Michel, H. (1998) *Proc. Natl. Acad. Sci. U.S.A. 95*, 12819−12824.
13. Oliveberg, M., Hallen, S., and Nilsson, T. (1991) *Biochemistry 30*, 436−440.
14. Mitchell, R., Mitchell, P., and Rich, P. R. (1992) *Biochim. Biophys. Acta 1101*, 188−191.
15. Mitchell, R., and Rich, P. R. (1994) *Biochim. Biophys. Acta 1186*, 19−26.
16. Babcock, G. T., and Wikström, M. (1992) *Nature (London) 356*, 301−309.
17. Hallen, S., and Nilsson, T. (1992) *Biochemistry 31*, 11853−11859.

18. Brzezinski, P., and Ädelroth, P. (1998) *J. Bioenerg. Biomembr. 30*, 99−107.
19. Paula, S., Sucheta, A, Szundi, I, and Einarsdottir, O. (1999) *Biochemistry 38*, 3025−3033.
20. Rich, P. R. (1995) *Aust. J. Plant Physiol. 22*, 470−486.
21. Ferguson, S. J., and Sorgato, (1982) *Annu. Rev. Biochem. 51*, 185−217.
22. Nicholls, D. G., and Ferguson, S. J. (1992) *Bioenergetics 2*, Academic Press, London.
23. Jasaitis, A., Verkhovsky, M. I., Morgan, J. E., Verkhovskaya, M. L., and Wikström, M. (1999) *Biochemistry 38*, 2697−2706.
24. Wikström, M., Morgan, J. E., and Verkhovsky, M. I. (1997) *Biochim. Biophys. Acta 1318*, 299−306.
25. Kannt, A., Lancaster, C. R. D., and Michel, H. (1998) *Biophys. J. 74*, 708−721.
26. Hinkle, P., and Mitchell, P. (1970) *Bioenergetics 1*, 45−60.
27. Ellis, W. R., Wang, H., Blair, D. F., Gray, H. B., and Chan, S. I. (1986) *Biochemistry 25*, 161−167.
28. Artzatbanov, V. Y., Konstantinov, A. A., and Skulachev, V. P (1978) *FEBS Lett. 87*, 180−185.
29. Mitchell, J. R., and Mitchell, P. (1989) *Biochem. Soc. Trans. 17*, 892−893.
30. Mitchell, R. (1991) Ph.D. Thesis, King's College, University of London, U.K.
31. Capitanio, N., Capitanio, G., De Nitto, E., and Papa, S. (1997) *FEBS Lett. 414*, 414−418.
32. Verkhovsky, M. I., Belevich, N., Morgan, J. E., and Wikström, M. (1999) *Biochim. Biophys. Acta 1412*, 184−189
33. Wikström, M., Bogachev, A., Finel, M., Morgan, J. E., Puustinen, A., Raitio, M., Verkhovskaya, M., and Verkhovsky, M. I. (1994) *Biochim. Biophys. Acta. 1187*, 106−111.
34. Morgan, J. E., Verkhovsky, M. I., and Wikström, M. (1994) *J. Bioenerg. Biomembr. 26*, 599−608.
35. Zaslavsky, D., Kaulen, A. D., Smirnova, I. A., Vygodina, T., and Konstantinov, A. A. (1993) *FEBS Lett. 336*, 389−393.
36. Konstantinov, A. A., Siletsky, S., Mitchell, D., Kaulen, A., and Gennis, R. B. (1997) *Proc. Natl. Acad. Sci. U.S.A. 94*, 9085−9090.
37. Antonini, G., Malatesta, F., Sarti, P., and Brunori, M. (1993) *Proc. Natl. Acad. Sci. U.S.A. 90*, 5949−5953.
38. Verkhovsky, M.. J., Jasaitis, A., Verkhovskaya, M. L., Morgan, J. E., and Wikström. M. (1999) *Nature 400*, 480−483.
39. Hendler, R. W., Pardhasaradhi, K., Reynafarje, B., and Ludwig, B. (1991) *Biophys. J. 60*, 415−423.
40. Lübben, M., Prutsch, A., Mamat, B., and Gerwert, K. (1999) *Biochemistry 38*, 2048−2056.
41. Puustinen, A., Bailey, J. A., Dyer, R. B., Mecklenburg, S. L., Wikström, M., and Woodruff, W. H. (1997) *Biochemistry 36*, 13195−13200.
42. Hellwig, P., Behr, J., Ostermeier, C., Richter, O.-M. H., Pfitzner, U., Odenwald, A., Ludwig, B., Michel, H., and Mäntele, W. (1998) *Biochemistry 37*, 7390−7399
43. Karpefors, M., Ädelroth, P., Aagaard, A., Sigurdson, H. E. M., and Brzezinski, P. (1998) *Biochim. Biophys. Acta 1365*, 159−169.
44. Jünemann, S., Meunier, B., Gennis, R. B., and Rich, P. R. (1997) *Biochemistry 36*, 14456−14464.
45. Vygodina, T. V., Pecoraro, C., Mitchell, D., Gennis, R. B., and Konstantinov, A. A. (1998) *Biochemistry 37*, 3053−3061.
46. Mills, D. A., and Ferguson-Miller, S. (1998) *Biochim. Biophys. Acta 1365*, 46−52.
47. Thomas, J. W., Lemieux, L. J., Alben, J. O., and Gennis, R. B. (1993) *Biochemistry 32*, 11173−11180.
48. Verkhovskaya, M. L., Garcia-Horsman, A., Puustinen, A., Rigaud, J. L., Morgan, J. E., Verkhovsky, M. I., and Wikström, M. (1997) *Proc. Natl. Acad. Sci. U.S.A. 94*, 10128−10131.
49. Riistama, S., Hummer, G., Puustinen, A., Dyer, R. B., Woodruff, W. H., and Wikström, M. (1997) *FEBS Lett. 414*, 275−280.
50. Watmough, N. J., Katsonouri, A., Little, R. H., Osborne, J. P., Furlongnickels, E., Gennis, R. B., Brittain, T., and Greenwood, C. (1997) *Biochemistry 36*, 13736−13742.
51. Ädelroth, P., Svensson-Ek, M., Mitchell, D. M., Gennis, R. B., and Brzezinski, P. (1997) *Biochemistry 36*, 13824−13829.
52. Rost, B., Behr, J., Hellwig, P., Richter, O.-M. H., Ludwig, B., Michel, H., and Mäntele, W. (1999) *Biochemistry 38*, 7565−7571.
53. Pfitzner, U., Odenwald, A., Ostermann, T., Weingard, L., Ludwig, B., and Richter, O. M. H. (1998) *J. Bioenerg. Biomembr. 30*, 89−97.
54. Gennis, R. B. (1998) *Biochim. Biophys. Acta 1365*, 241−248.
55. Wilson, D. F., Lindsay, J. G., and Brocklehurst, S. E. (1972) *Biochim. Biophys. Acta 256*, 277−286.
56. Sucheta, A., Szundi, I., and Einarsdottir, O. (1998) *Biochemistry 37*, 17905−17914.
57. Fann, Y. C., Ahmed, I., Blackburn, N. J., Boswell, J. S., Verkhovskaya, M. L., Hoffmann, B. M., and Wikström, M. (1995) *Biochemistry 34*, 10245−10255.
58. Cheesman, M. R., Watmough, N. J., Gennis, R. B., Greenwood, C., and Thomson, A. J. (1994) *Eur. J. Biochem. 219*, 595−602.
59. Sacks, V., Marantz, Y., Aagaard, A., Checover, S., Nachliel, E., and Gutman, M. (1998) *Biochim. Biophys. Acta 1365*, 232−240.
60. Chance, B., Saronio, C., and Leigh, J. S. (1975) *J. Biol. Chem. 250*, 9226−9237.
61. Weng, L., and Baker, G. M. (1991) *Biochemistry 30*, 5727−5733.
62. Proshlyakov, D. A., Ogura, T., Shinzawa-Itoh, K., Yoshikawa, S., and Kitagawa, T. (1996) *Biochemistry 35*, 8580−8586.
63. Kitagawa, T., and Ogura, T. (1997) in *Progress in Inorganic Chemistry*, (Karlin, K. D., Ed.) Vol. 45, pp 431−479, Wiley, New York.
64. Proshlyakov, D. A., Pressler, M. A., and Babcock, G. T. (1998) *Proc. Natl. Acad. Sci. U.S.A. 95*, 8020−8025.
65. Zaslavsky, D. L., Smirnova, I. A., Ädelroth, P., Brzezinski, P., and Gennis, R. B. (1999) *Biochemistry 38*, 2307−2311.
66. Moody, A. J., and Rich, P. R. (1994) *Eur. J. Biochem. 226*, 731−737.
67. Fabian, M., and Palmer, G. (1995) *Biochemistry 34*, 13802−13810.
68. Michon, T., Chenu, M., Kellershon, N., Desmadril, M., and Gueguen, J. (1997) *Biochemistry 36*, 8504−8513.
69. MacMillan, F., Kannt, A., Behr, J., Prisner, T., and Michel, H. (1999) *Biochemistry 38*, 9179−9184.
70. Wilson, M. T., Jensen, P., Aasa, R., Malmström, B. G., and Vänngård, T. (1982) *Biochem. J. 203*, 483−492.
71. Han, S., Ching, Y. C., and Rousseau, D. L. (1990) *Nature 348*, 89−90.
72. Jünemann, S., Meunier, B., Fisher, N., and Rich, P. R. (1999) *Biochemistry 38*, 5248−5255.
73. Kannt, A., Soulimane, T., Buse, G., Becker, A., Bamberg, E., and Michel, H. (1998) *FEBS Lett. 434*, 17−22.
74. Behr, J., Hellwig, P., Mäntele, W., and Michel, H. (1998) *Biochemistry 37*, 7400−7406.
75. Karpefors, M., Ädelroth, P., Zhen, Y., Ferguson-Miller, S., and Brzezinski, P. (1998) *Proc. Natl. Acad. Sci. U.S.A. 95*, 13606−13611.
76. Siletsky, S., Kaulen, A. D., and Konstantinov, A. A. (1999) *Biochemistry 38*, 4853−4861.
77. Rich, P. R., Jünemann, S., and Meunier, B. (1998) *J. Bioenerg. Biomembr. 30*, 131−138.
78. Morgan, J. E., Verkhovsky, M. I., and Wikström, M. (1996) *Biochemistry 35*, 12235−12240.

BI9910934